Owolabi et al. International Journal of Mechanical and Materials Engineering (2016) 11:3
DOI 10.1186/s40712-016-0056-0

International Journal of Mechanical and Materials Engineering
a SpringerOpen Journal

ORIGINAL ARTICLE Open Access

Dynamic response of acrylonitrile butadiene styrene under impact loading

Gbadebo Owolabi[1*], Alex Peterson[1], Ed Habtour[2], Jaret Riddick[2], Michael Coatney[2], Adewale Olasumboye[1] and Denzell Bolling[1]

Abstract

Background: The goal of the study is to understand the potential energy absorption benefits ofcomponents fabricated using fused deposition modeling additive manufacturing under high strain rateloading.

Methods: Tensile tests were conducted on 3-D printed acrylonitrile butadiene styrene (ABS) at differentstrain rates, according to the ASTM D638 standard, to assess its strain rate sensitivity under quasi-staticloads. The tensile test was also necessary to determine the mechanical properties necessary to characterizethe dynamic response of the ABS at high strain rates. The ABS specimens were subjected to high strainrate deformation through the use of the split Hopkinson pressure bar.

Results: During compression, a new phenomenon described as a multistage collapse in which the samplesundergo multiple stages of contraction and expansion was observed as the impact load was applied. Thismultistage deformation behavior may be attributable to the ring formed around layers in the specimen dueto the manner of fabrication which potentially absorbed and released the energy, thus acting as a multistage spring. As the velocity of impact increases, it is observed that the ABS capability for energy absorption decreased to where there was only one stage of compression equivalent to the initial stage.

Conclusion: The multistage collapse of the 3-D printed ABS specimen indicates a potential for a novel energy absorption mechanism to be exploited at lower strain rates. Future work in the area should include more studies about printing orientation, as well as investigating the impact of the presence of the outer cylindrical ring on the overall dynamic response.

Keywords: Additive manufacturing, Acrylonitrile butadiene styrene, High strain rates, Dynamic response

Background

Through the use of direct digital manufacturing (DDM), more commonly known as additive manufacturing (AM), various thermoplastics can be used as the basis for creating models and to be printed for a vast amount of applications that could potentially be beneficial with respect to the design and manufacturing of mechanical and structural components. Using this approach, acrylonitrile butadiene styrene (ABS) can be printed at various orientations, and the understanding of the effect that this process has on their behavior under service loads could lead to potential benefits that were previously unexplored. DDM uses a combination of computer-aided design (CAD) and computer-aided manufacturing (CAM) as well as computer codes designed to interface with advanced 3-D additive manufacturing prototyping machines to produce a desired component (Yan and Gu 1996).

This study explores the fused deposition modeling (FDM) and the printing orientation as a means to quantify the potential benefits of AM to allow for a more cost-effective, time-efficient, in-house fabrication of designs, while optimizing the mechanical and structural integrity. In FDM, CAD software is used to convert a file containing a 3-D model into 3-D stereolithography (STL) format. The STL file is imported into a CAM software, which produces a physical replica of the 3-D model sliced into thin layers comprised of tool paths used by the 3-D printing machine to place continuous feedstock filament comprised of ABS

* Correspondence: gbadebo.owolabi@howard.edu
[1]Department of Mechanical Engineering, Howard University, Washington, DC, USA
Full list of author information is available at the end of the article

and onto a surface to build up the 3-D component layer-by-layer (Riddick et al.). Advanced 3-D additive manufacturing prototyping (3-D printing) has been used in a variety of applications, which include medical designs, oil filter assemblies, prototypes, replacement parts, and dental crowns (Berman 2012).

In the design of mechanical and structural components, it is essential to understand the mechanical behavior at different loading rates based on the desired applications. The present investigation is aimed at understanding the effect of high strain rate loading (>10^2 s^{-1}) on the dynamic response of ABS for potential benefits in energy absorption in mechanical and structural applications. Riddick, et al. (Riddick et al.) characterized the effects of varying build direction and raster orientation on the strength and stiffness of ABS fabricated by FDM. Results of the experimental characterization show that rasters formed parallel to the loading direction fabricated in the through-the-thickness direction yielded the highest strength and modulus at 34.17 MPa and 2.79 GPa, respectively. The overall results clearly indicated anisotropy in the macroscale response due to raster orientation and build direction with respect to the load axis. In the area of high strain rate deformation, there has been extensive work on understanding the effects of high strain rate on metals such as aluminum alloys, steels, and other metals (Smerd et al. 2005; Djapic Oosterkamp et al. 2000; Odeshi et al. 2006; Lee and Lin 1998). Many experiments on dynamic response of metals have been conducted through the usage of the split Hopkinson pressure bar (SHPB) for strain rates greater than 10^2 (Kuhn and Dana 2000). Very limited exploratory research has, however, been conducted on the dynamic response of polymers, more specifically ABS. The range of interest for the present study (10^2–10^3) is within the capability of the SHPB test apparatus making this setup suitable for completing the experiments required to investigate the dynamic response of ABS at high strain rates.

When observing metals at high strain rates, one of the main relationships that are analyzed is the relationship between the stress that a material undergoes and the strain as the strain rate is increased. Yazdani et al. (2009); Qiang et al. (2003); Lee et al. (2005) conducted studies on the dynamic deformation of copper and titanium alloys and observed that the maximum stress did not change drastically with increasing strain rates. Siviour et al. (2006) showed that the final strain achieved for polymers was directly related to the strain rate applied. For polymers, such as ABS, the mechanical properties vary considerably from those observed in metals. Gaining a better understanding of the strain rate dependency of ABS will help in effectively determining the stress limits for a given design application as a function of the strain rate.

Mulliken and Boyce (2006) performed studies on characterizing the strain rate dependency of polymers from 10^{-4} to 10^4 s^{-1}. The results demonstrated that an increase in strain rate sensitivity was observed at elevated loading rates compared to those observed for quasi-static loading. Wally and Field (1994) conducted multiple tests on the strain rate sensitivity of polymers subjected to loads ranging from quasi-static to high strain rates. Samples were formed using a solid ABS block to determine the mechanical property at various strain rates (Fig. 1). Through the analysis of the solid ABS, a linear relationship between the strain rate applied and the maximum stress observed in the quasi-static region was observed (Walley and Field 1994). As the transitional phase from quasi-static to dynamic loading is reached, there is a drastic change in the increase in the gradient of the slope. Unlike observations of adiabatic conditions occurring in metals, there is no drastic change in temperature.

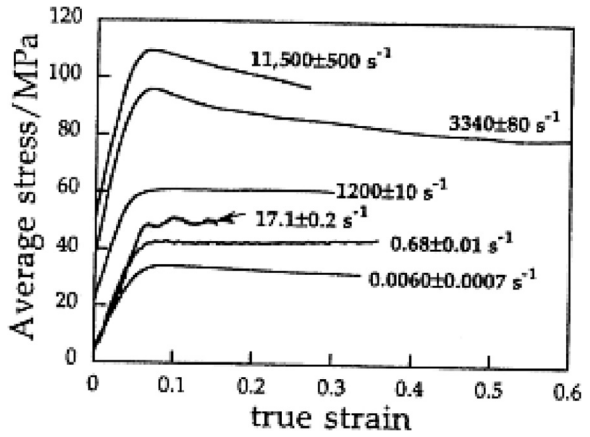

Fig. 1 Solid ABS stress-strain curve (Walley and Field 1994)

The novelty of the present research is that rather than testing a solid block of ABS, machined down to the appropriate size, here, an advanced 3-D additive manufacturing approach is used to print the specimens. Artifacts of the 3-D printing process coincidentally create logical structures for energy absorption. Recent research in multifunctional structures seeks to draw upon bio-mimicry to produce graceful progression to plasticity through unique damage absorption. Malkin et al. (2013) have considered the discontinuous reinforcement phases in high-toughness composite nacre as an inspiration to introduce a degree of pseudo-ductility to fiber-reinforced polymer. By introducing ply cuts of various spacings and densities to exploit discontinuities inspired by architectures of nacre found in nature, pseudo-ductility characterized by graceful collapse phenomenon was achieved. Sen and Buehler (2010) demonstrated a bottom-up systematic approach rooted in atomistic modeling to investigate enhanced defect tolerance in hierarchical structures fabricated from brittle material. Stable crack propagation resistance due to structural hierarchy was shown to enable toughness of otherwise brittle

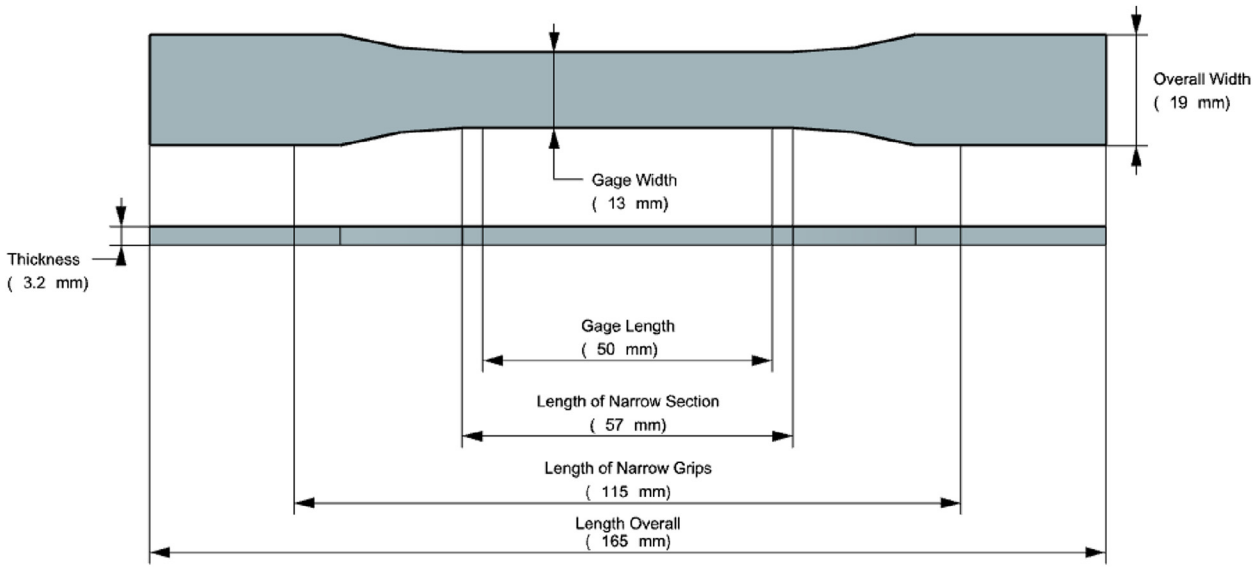

Fig. 2 ASTM D638-03 dog bone (International et al. 2004)

base material, traditionally highly sensitive to small nano-scale defects. Dyskin et al. (2003) proposed a new materials design concept in which regular assemblies of topologically interlocked elements are the basis for strong flexible composite materials with high impact resistance. The behavior that Dyskin et al. (2003) confirmed in layers formed of topologically interlocked elements composed of aluminum alloy material is an example of pseudo-ductile behavior.

Khandelwal et al. (2012) fabricated cellular topologically interlocking material (TIM) composed of tetrahedral elements using FDM additive manufacturing of ABS plastic. Impact tests demonstrated that the cellular TIMs composed of intrinsically brittle base material exhibited perfect softening behavior. The experimental results exhibit a positive correlation between strength and toughness, which is a clear demonstration of pseudo-ductile behavior. It is

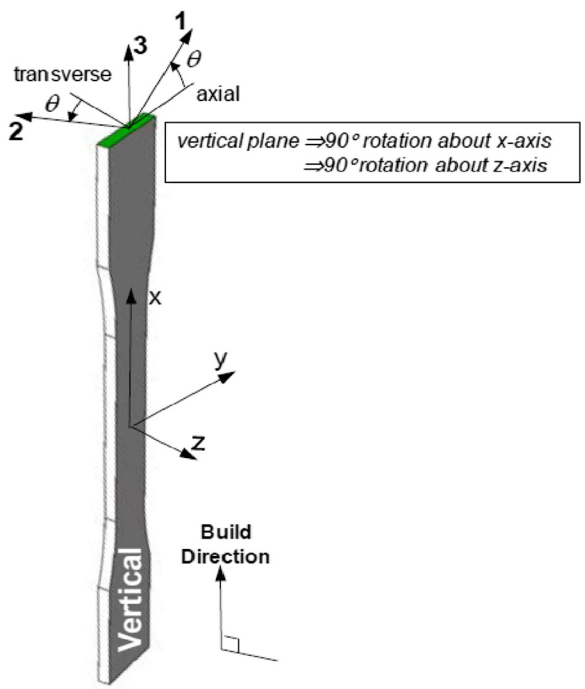

Fig. 3 Material build direction 0/90 orientation

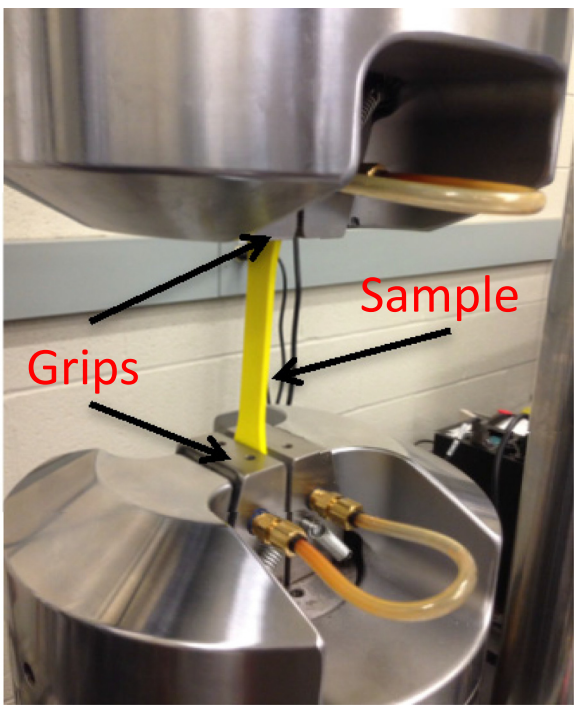

Fig. 4 Experimental setup prior to testing

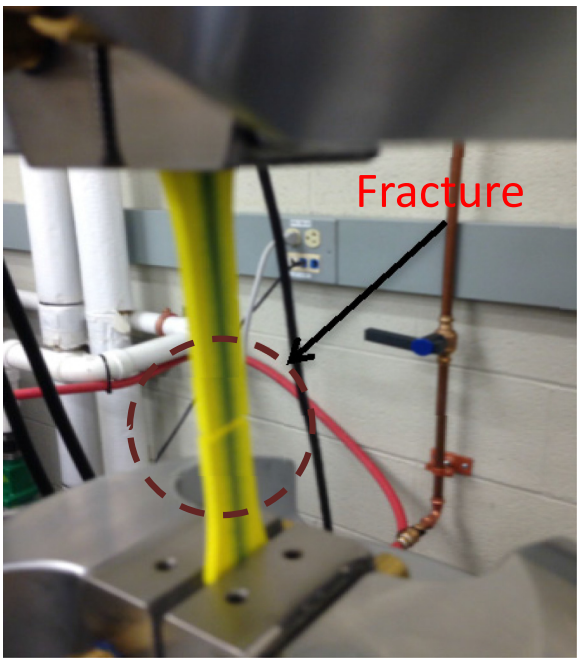

Fig. 5 Experimental setup after testing

desirable to understand whether the potential benefits of 3-D printed polymer can be harnessed for use in novel mechanical and structural applications. The present study explores FDM-printed materials to quantify the potential benefits to dynamic response of structures such as TIMs to understand the potential effect on cost-effective, time-efficient designs optimized for mechanical strength and structural integrity. The primary long-term research goal is to formulate concepts for material performance beyond present capability to enable new approaches to highly optimized and multifunctional structural designs.

Experimental Method

Before experiments at high strain rates were conducted, it was essential to understand how the material will behave under quasi-static loading condition. This interest arises from the fact that majority of polymers are strain rate sensitive, i.e., the maximum stress observed in an object before deformation, or failure, is directly related to strain rate. It can be noticed in Fig. 1 that over a wide range of strain rates, there were different levels of maximum stress observed in the ABS throughout the experiments. In order to understand the tensile properties of the 3-D printed ABS, preliminary tensile tests were conducted using the ASTM D638-03 Standard Test Method for Tensile Properties of Plastics. The standard recommends a type I specimen for rigid and semi rigid plastics (International et al. 2004). The type I specimen dimensions used in the tensile testing are shown in Fig. 2.

When designing the specimen for tensile testing, it is important that the tensile specimen is built such that the orientation of the tensile test loads is the same as that for the subsequent dynamic tests. The tensile specimen was built with each successive layer composed of 0° and 90° orientations built from the ground up, as shown in Fig. 3. According to the ASTM D638-03 standard (International et al. 2004), the test specimen is to be tested at a minimum displacement rate of 0.50 cm/min to extract the material properties such as the yield point, the elastic modulus, and the ultimate tensile strength. Using this as a starting point and in order to understand if the material was strain rate-dependent, experiments were performed at displacement rates of 0.5, 5, 25, 35, and 50 cm/min. Figures 4 and 5 show the specimen before and after testing was conducted.

Once the tensile testing was completed, the next phase in the material design and testing was the dynamic

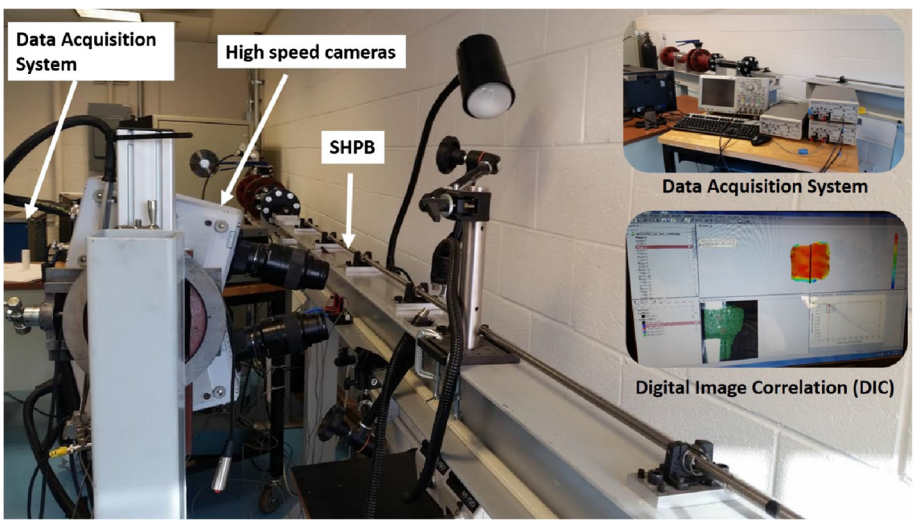

Fig. 6 Photographs of the split Hopkinson pressure bar synchronized with data acquisition and digital image correlation systems

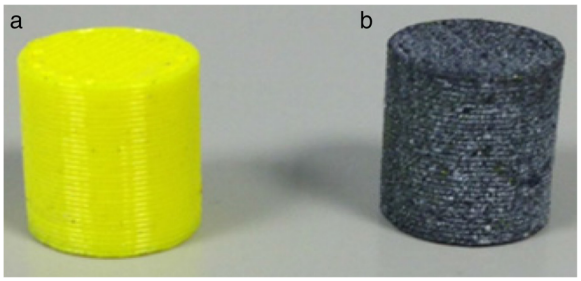

Fig. 7 **a** Unpainted specimen. **b** Painted specimen

compression loading at high strain rates. The specimens for the high strain rate compression test were 8 mm long and 8 mm in diameter. The compressive loading was conducted using the conventional SHPB shown in Fig. 6. The setup comprised of a gas gun connected to a striker bar that induced a velocity into the system. The impact velocity was then transferred to an incident bar which had a strain gage attached to it to capture the dynamic response as a result of the applied compression on the specimen. The reflected waves from the specimen were captured through the same strain gage that recorded the incident waves. On the other side of the specimen was the transmitted bar which captured the waves that were transmitted through the specimen as a result of the compressive loading. The measurements were then relayed from the strain gage to an oscilloscope, which provided the output signals. The signals were converted into time-domain stress, strain, displacement, force, and strain rate. Finally, these parameters were used to consider the dynamic response of the ABS cylindrical specimen under high strain rates.

In conjunction with the data captured through the use of the strain gages and the oscilloscope, the material deformation was also captured at the same time by utilizing high-speed digital image correlation (DIC) cameras, shown in Fig. 6, which captured the compression at a frame rate of 124,000 frames per second (fps). The DIC code was subsequently utilized to capture the displacements of selected points along the load axis as a result of deformation by tracking dots that were applied through spray painting patterns of black and white along the length of the specimen. A comparison between the plain and the spray-painted specimens is shown in Fig. 7. It is important to note that the cylindrical specimens are fabricated by FDM in a layer-by-layer manner. Each layer is formed by printing a circular ring of material and then filling in the ring in a serpentine fashion. The result of this manner of fabrication is a support ring built around layers of 3-D printed material, each layer alternating perpendicularly in the plane of the circular cross-section (normal to the load direction).

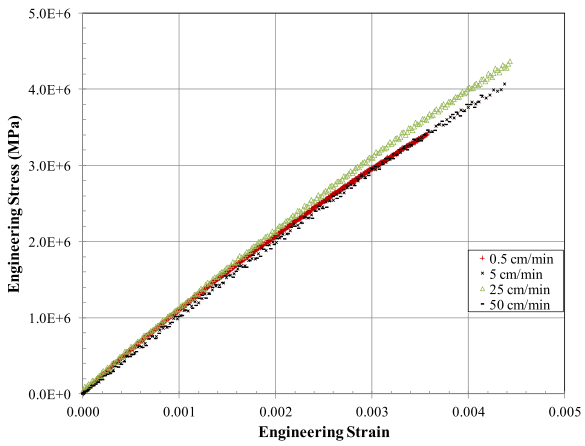

Fig. 8 Stress-strain curve at various strain rates

Table 1 Tensile testing results

Displacement rate	Maximum stress (MPa)	Elastic modulus (GPa)
0.5 cm/min	3.4	1.0
5 cm/min	4	0.9
25 cm/min	4.3	1.0
50 cm/min	3.9	1.0
Average	3.9	0.975

Results and discussion

The mechanical testing on the ABS specimen was accomplished in two different stages. Tensile testing was first conducted to study the strain rate dependency of the ABS and to obtain the mechanical properties that are required to determine the pressure corresponding to a desired impact velocity during high strain rate testing. ABS samples were then tested at strain rates from 500 to 2000 s^{-1}.

Tensile test results

Figure 8 shows the stress-strain curve from the tensile testing at various displacement rates. Table 1 shows the specimen testing rates for strain rate dependency, in accordance with ASTM D638-03 standards. It was observed that the 3-D printed ABS material was brittle; thus,

Table 2 Strain rate, pressure, and velocity of impact

ABS 8 × 8 mm^2 cylindrical specimen			ABS 10 × 10 mm^2 cylindrical specimen		
Strain rate (s^{-1})	Velocity (m/s)	Pressure (kPa)	Strain rate (s^{-1})	Velocity (m/s)	Pressure (kPa)
500	4.096	20.68	500	5.154	26.82
750	6.097	32.96	750	7.656	44.61
1000	8.097	48.33	1000	10.158	68.19
1500	12.097	91.08	1500	15.162	114.80
2000	16.098	150.86	2000	20.165	224.84

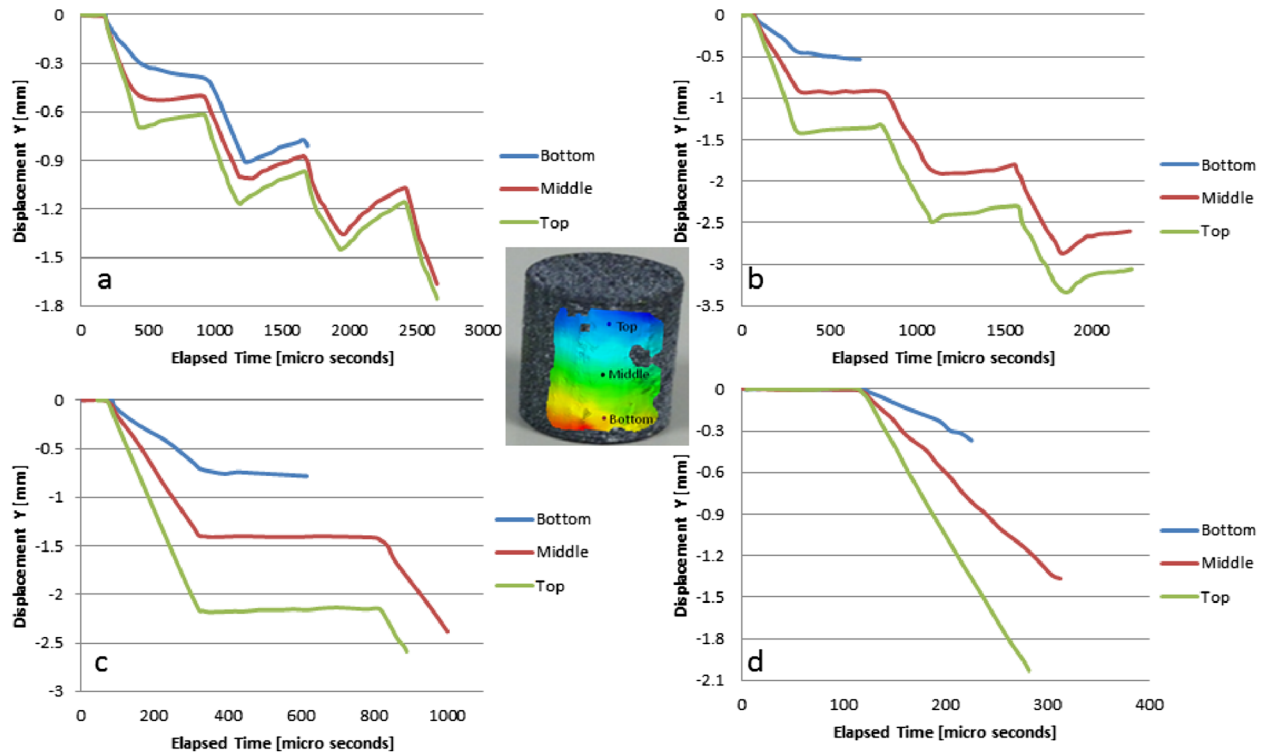

Fig. 9 Longitudinal stage displacement at different strain rates. **a** 500 s^{-1}. **b** 1000 s^{-1}. **c** 1500 s^{-1}. **d** 2000 s^{-1}

evidence of plastic deformation was not apparent in the tensile experiments, which was directly related to the manner in which the material was built. The specimens experienced tensile stress between 3.4 to 4.8 MPa prior to fracture for strain rates of 0.5 to 50 cm/min, respectively, as shown in Fig. 8. However, the modulus of elasticity appeared to be consistent among the specimens, as shown in Table 1.

Dynamic compression tests results

The average maximum stress from the tensile test results was used in a MATLAB code to determine the applied pressure corresponding to the targeted impact velocities for various strain rates to which the samples were subjected to as shown in Table 2.

Figure 9 shows the deformation observed due to compression with respect to time, where Y is the longitudinal displacement. The results showed that at lower strain rates, there were different stages of deformation observed while the specimen underwent one initial impact. Using the DIC, the deformation evolutions at three different points, i.e., the top, the middle, and the bottom location reference points, were captured and analyzed as the specimens were impacted at different strain rates as shown in Fig. 9. At a strain rate of 500 s^{-1}, compression was not evident until about 200 μs as shown in Fig. 9a. Beyond this stage, however, the compression began and the specimen contracted longitudinally. Towards the end of this stage, the material expanded slightly noting that the overall displacement increased until the next stage of contractions occurred. As the induced strain rate increased, the stages of deformation decreased until eventually there was only one stage at 2000 s^{-1} as shown in Fig. 9b–d. The displacements observed by the system were also evident in the compression video captured by the high-speed cameras. This phenomenon of multistage contraction and expansion may be due to the support ring built around the 3-D printed material, which holds the perpendicular layers in place, beginning to absorb and displace energy acting as a multistage spring. Once the outer ring reached its maximum limit of energy absorption, it collapsed and the energy was transferred to the

Table 3 Specimen Height

Strain rate	Initial height (mm)	Average final height (mm)
500	8	8.11
750	8	7.95
1000	8	7.18
1500	8	5.85
2000	8	4.07

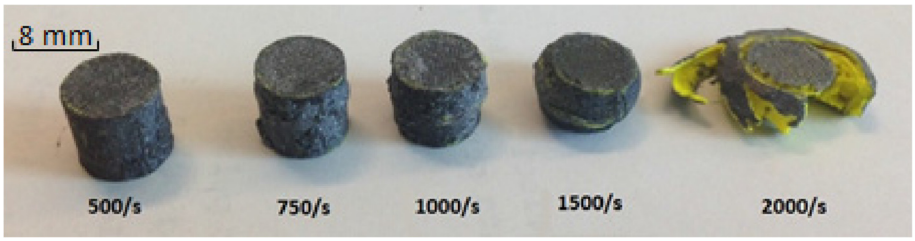

Fig. 10 Specimen deformation

perpendicular layers causing a complete fracture of the sample at 2000 s^{-1}.

Table 3 shows the initial height of the specimen before deformation in comparison to the final height. Interestingly, at the lowest strain rate of 500 s^{-1}, the specimen shows signs of actually expanding after the compression process was completed. Once a strain rate of 750 s^{-1} was reached, the average final height began gradually to decrease, and from this strain rate, failure began to occur by buckling until complete fracture was observed. At a strain rate of 2000 s^{-1}, the specimen underwent about a 60 % reduction in size, which was the strain rate at which fracture occurred. The damage evolution of the specimen started to become drastic once the applied strain rate exceeded 1000 s^{-1}, as shown in Fig. 10 which provides the images of the specimens after testing.

The specimen failure as a function of the strain rate can be divided into two different strain rate ranges: the first consisting of strain rate from 500 to 1000 s^{-1} and the second consisting of the final two strain rates 1500 and 2000 s^{-1} as shown in Fig. 11. As the transition from one strain range to the other occurred, the corresponding yield point changed along with the maximum stress. For a strain rate of 1500 s^{-1} the yield point and the maximum stress were 91.6 and 93.1 MPa, respectively. For the strain rate of 2000 s^{-1}, yielding occurred at 89.70 MPa and the maximum stress was 96.70 MPa. In this range of strain rate, there was also significant stress drop, followed by strain hardening and then a drastic decrease in stress as a result of stress collapse.

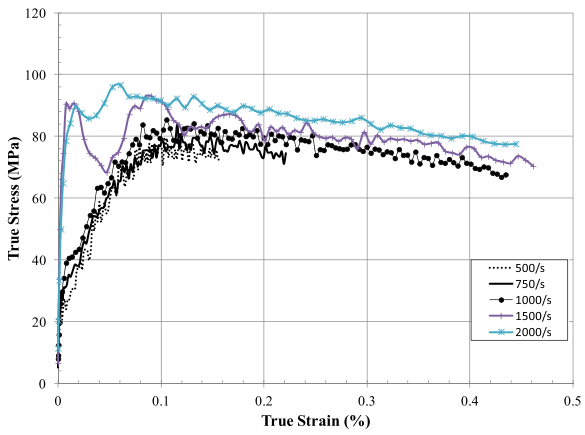

Fig. 11 Stress-strain curve under dynamic compression loading at various strain rates

Conclusions

The present study presents the results of exploratory studies conducted to understand the effect of 3-D printing on the response of ABS polymer under dynamic loading. At strain rates above 1000 s^{-1} applied using the split Hopkinson pressure bar experiment, failure begins to occur in the printed ABS by buckling characterized by increasing height reduction and crushing as the strain rate increases beyond 1000 s^{-1} up to complete failure at 2000 s^{-1}. Below the 1000 s^{-1} limit, there is minimal height reduction or evidence of failure observed. At the lower strain rates, images captured through the use of the DIC system indicate iterative contraction and expansion of the material as the incident load is applied. The iterative behavior may be due to the support ring built around the 3-D printed material, which holds the perpendicular layers in place, beginning to absorb and displace energy acting as a multistage spring. The dynamic results indicate that the specimen shows a linear relationship between the true stress and the true strain up to its yield point. The highest plastic deformation is observed at higher strain rates along with higher levels of stress. However, as the strain rate is increased, there is more evidence of stress collapse ultimately leading to the failure of the specimens. The multistage collapse of the 3-D printed ABS specimen indicates a potential for a novel energy absorption mechanism to be exploited at lower strain rates. Future work in the area should include more studies about printing orientation, as well as investigating the impact of the presence of the outer cylindrical ring on the overall dynamic response.

Competing interests
The authors declare that they have no competing interests.

Authors' contributions
All authors read and approved the final manuscript.

Acknowledgements
The authors are grateful for the financial support provided by the Department of Defense (DOD) through the research and educational program for HBCU/MSI (contract # W911NF-12-1-061) monitored by Dr. Asher A. Rubinstein (Solid Mechanics Program Manager, ARO). Alex Peterson is also grateful for the summer financial support provided via the College Qualified Program sponsored by the American Society of Engineering Education and the DOD that gives interested students, both undergraduate and graduate level, the opportunity for research internship in the DOD labs.

Author details
[1]Department of Mechanical Engineering, Howard University, Washington, DC, USA. [2]US Army Research Lab, Vehicle Technology Directorate, Aberdeen Proving Ground, Aberdeen, MD, USA.

Received: 22 December 2015 Accepted: 8 March 2016
Published online: 16 March 2016

References

ASTM International. (2004). *Standard test method for tensile properties of plastics, Standard D 638-03* (pp. 1–15).
Berman, B. (2012). 3-D printing: the new industrial revolution. *Business Horizons., 55*, 155–162.
Djapic Oosterkamp, L., Ivankovic, A., & Venizelos, G. (2000). High strain rate properties of selected aluminium alloys. *Materials Science and Engineering: A., 278*, 225–235.
Dyskin, A. V., Estrin, Y., Kanel-Belov, A. J., & Pasternak, E. (2003). A new principle in design of composite materials: reinforcement by interlocked elements. *Composites Science and Technology., 63*, 483–491.
Khandelwal, S., Siegmund, T., Cipra, R. J., & Bolton, J. S. (2012). Transverse loading of cellular topologically interlocked materials. *International Journal of Solids and Structures., 49*, 2394–2403.
Kuhn, H., & Dana, M. (2000). *ASM handbook: mechanical testing and evaluation* (pp. 462–476). Materials Park, OH: The Materials Information Society.
Lee, W.-S., & Lin, C.-F. (1998). Plastic deformation and fracture behaviour of Ti–6Al–4V alloy loaded with high strain rate under various temperatures. *Materials Science and Engineering A, 24*, 48–59.
Lee, D.-G., Kim, Y. G., Nam, D.-H., Hur, S.-M., & Lee, S. (2005). Dynamic deformation behavior and ballistic performance of Ti–6Al–4V alloy containing fine α2 (Ti3Al) precipitates. *Materials Science and Engineering: A, 391*, 221–234.
Malkin, R., Yasaee, M., Trask, R. S., & Bond, I. P. (2013). Bio-inspired laminate design exhibiting pseudo-ductile (graceful) failure during flexural loading. *Composites Part A: Applied Science and Manufacturing., 54*, 107–116.
Mulliken, A. D., & Boyce, M. C. (2006). Mechanics of the rate-dependent elastic–plastic deformation of glassy polymers from low to high strain rates. *International Journal of Solids and Structures., 43*, 1331–1356.
Odeshi, A. G., Al-ameeri, S., Mirfakhraei, S., Yazdani, F., & Bassim, M. N. (2006). Deformation and failure mechanism in AISI 4340 steel under ballistic impact. *Theoretical and Applied Fracture Mechanics., 45*, 18–24.
Qiang, L., Yongbo, X., & Bassim, M. N. (2003). Dynamic mechanical properties in relation to adiabatic shear band formation in titanium alloy-Ti17. *Materials Science and Engineering: A, 358*, 128–133.
Riddick J, Hall A, Haile M, Von Wahlde R, Cole D, and Biggs S. Effect of manufacturing parameters on failure in acrylonitrile-butadiane-styrene fabricated by fused deposition modeling, In 53rd ASME/ASME/ASCE/AHS/ASC Structures, Structural Dynamics and Materials Conference 20th ASME/ASME/AHS Adaptive Structures Conference 14th ASME.
Sen, D., & Buehler, M. J. (2010). Atomistically-informed mesoscale model of deformation and failure of bioinspired hierarchical silica nanocomposites. *International Journal of Applied Mechanics., 2*, 699–717.
Siviour, C. R., Walley, S. M., Proud, W. G., & Field, J. E. (2006). Mechanical behaviour of polymers at high rates of strain. *Journal De Physique IV., 134*, 949–955.
Smerd, R., Winkler, S., Salisbury, C., Worswick, M., Lloyd, D., & Finn, M. (2005). High strain rate tensile testing of automotive aluminum alloy sheet. *International Journal of Impact Engineering., 32*, 541–560.
Walley, S. M., & Field, J. E. (1994). Strain rate sensitivity of polymers in compression from low to high rates. *Dymat Journal., 1*, 211–227.
Yan, X., & Gu, P. (1996). A review of rapid prototyping technologies and systems. *Computer-Aided Design., 28*, 307–318.
Yazdani, F., Bassim, M. N., & Odeshi, A. G. (2009). The formation of adiabatic shear bands in copper during torsion at high strain rates. *Procedia Engineering., 1*, 225–228.